2008 American Control Conference
Westin Seattle Hotel, Seattle, Washington, USA
June 11-13, 2008

Neuroadaptive Output Feedback Control for Automated Anesthesia with Noisy EEG Measurements

Wassim M. Haddad, Konstantin Y. Volyanskyy, and James M. Bailey

Abstract— **Critical care patients, whether undergoing surgery or recovering in intensive care units, require drug administration to regulate physiological variables such as blood pressure, cardiac output, heart rate, and degree of consciousness. The rate of infusion of each administered drug is critical, requiring constant monitoring and frequent adjustments. Nonnegative and compartmental models provide a broad framework for biological and physiological systems, including clinical pharmacology, and are well suited for developing models for closed-loop control of drug administration. In this paper, we develop a neuroadaptive output feedback control framework for nonlinear uncertain nonnegative and compartmental systems with nonnegative control inputs and noisy measurements. In addition, the neuroadaptive controller guarantees that the physical system states remain in the nonnegative orthant of the state space. Finally, the proposed approach is used to control the infusion of the anesthetic drug propofol for maintaining a desired constant level of depth of anesthesia for noncardiac surgery in the face of noisy electroencephalographic (EEG) measurements.**

I. Introduction

The dosing of most drugs is a process of empirical administration of a low dose with observation of the biological effect and subsequent adjustment of the dose in the hopes of achieving the desired effect. This is true of anesthetic drugs, just as it is of chronically administered medications (for example, anti-hypertensive agents). In the acute environment of the operating room and intensive care unit (ICU), this can result in inefficient, and possibly even dangerous, titration of drug to the desired effect. There has been a long interest in use of the electroencephalograph (EEG) as an objective, quantitative measure of consciousness that could be used as a performance variable for closed-loop control of anesthesia. Ever since the pioneering work of Bickford [1], it has been known that the EEG changes with the induction of anesthesia. Processed electroencephalogram (EEG) algorithms have been extensively investigated as monitors of the level of consciousness in patients requiring surgical anesthesia [1], [2]. However, the EEG is a complex of multiple time series and in earlier work it was difficult to identify one single aspect of the EEG signal that correlated with the clinical signs of anesthesia.

Subsequent to this early research there has been substantial progress in the development of processed EEG monitors that analyze the raw data to extract a single measure of the depth of anesthesia. The best known of these monitors is the bispectral or BIS monitor, which calculates a single composite EEG measure that is well correlated with the depth of anesthesia [3]. The BIS signal ranges from 0 (no cerebral electrical activity) to 100 (the normal awake state). Available evidence indicates that a BIS signal less than 55 is associated with lack of consciousness. While BIS monitoring has proven useful in the operating room environment, there have been inconsistencies reported and attempts to extend BIS monitoring for the evaluation of sedation outside of the operating room have been unsuccessful [4]. One of the key reasons for this is due to the fact that the signal-averaging algorithm within the BIS monitor ignores signal noise, and when there is excessive noise, the BIS monitor does not generate a signal.

It is widely appreciated that BIS monitoring, or for that matter, any EEG monitoring, can be fraught with error because of the potential for outside interference to produce an unfavorable signal-to-noise ratio yielding spurious results. Nonphysiologic artifactual signals may be generated from sources external to the patient that include lights, electric cautery devices, ventilators, pacemakers, patient warming systems, and electrical noise related to the many different kinds of monitors normally found in an operating room or ICU. Physiologic movements such as eye movements, myogenic activity, perspiration, and ventilation can produce artifactual increases in the BIS score. In particular, it is apparent that electromyographic (EMG) activity can spuriously increase the BIS score [5]. The co-administration of neuromuscular blockade eliminates artifacts from muscle movement, which can be superimposed on the BIS score; and this undoubtedly contributes to the widespread use and value of the BIS device during surgery. However, to extend this technology outside of the operating room, or for that matter, to nonparalyzed patients in the operating room, further refinements are needed. In addition, if the BIS signal is to be used to quantify levels of consciousness for feedback control in general anesthesia, then observation noise needs to be accounted for in the control system design process.

The challenge to the use of the BIS signal for closed-loop control of anesthesia is that the relationships between drug dose and tissue concentration (pharmacokinetics) and between tissue concentration and physiological effect (pharmacodynamics) is highly variable between individuals. In addition, observation noise in the BIS signal results in feedback measurement signals with high signal-to-noise ratios that need to be accounted for in the control algorithm. Adaptive feedback controllers seem particularly promising given this inter-patient variability as well as BIS signal variation due to noise. In previous work, we have used nonnegative and compartmental dynamical systems theory to develop adaptive and neuroadaptive controllers for controlling the depth of anesthesia [6]–[8]. One of our initial efforts was the development of a direct adaptive control framework for uncertain nonlinear nonnegative and compartmental systems with nonnegative control inputs [6], [7]. This framework is Lyapunov-based and guarantees partial asymptotic set-point regulation, that is, asymptotic setpoint stability with respect to part of the closed-loop system states associated with the physiological state variables. In addition, the adaptive controllers, which are constructed without requiring knowledge of the pharmacokinetic and pharmacodynamic parameters,

This research was supported in part by the National Science Foundation under Grant ECS-0601311.

W. M. Haddad and K. Y. Volyanskyy are with the School of Aerospace Engineering, Georgia Institute of Technology, Atlanta, GA 30332-0150, USA (wm.haddad@aerospace.gatech.edu), (gtg891s@mail.gatech.edu).

James M. Bailey is with Northeast Georgia Medical Center, Gainsville, GA 30503, USA (james.bailey@nghs.com).

provide a nonnegative control input for stabilization with respect to a given setpoint in the nonnegative orthant. Subsequently, we also developed a neuroadaptive output feedback control framework for uncertain nonlinear nonnegative and compartmental systems with nonnegative control inputs [8]. This framework is also Lyapunov-based and guarantees ultimate boundedness of the error signals corresponding to the physical system states in the face of inter-patient pharmacokinetic and pharmacodynamic variability.

In a recent paper [9] we presented numerical and clinical results that compares and contrasts our adaptive control algorithm with our neural network adaptive control algorithm for controlling the depth of anesthesia in the operating theater during surgery. Specifically eleven clinical trials were performed with our adaptive control algorithm [7] and seven clinical trials were performed with our neural network algorithm [8] at the Northeast Georgia Medical Center in Gainesville, Georgia. The proposed automated anesthesia controllers demonstrated excellent regulation of unconsciousness and allowed for a safe and effective administration of the anesthetic agent propofol. However, the adaptive and neuroadaptive controllers presented in [9] did not account for measurement noise in the EEG signal. Clinical testing has clearly demonstrated the need for developing adaptive and neuroadaptive controllers that can address system measurement noise [9]. In this paper, we extend the neuroadaptive controller framework developed in [8] to address measurement noise in the BIS signal for feedback control.

II. Mathematical Preliminaries

In this section, we introduce notation, several definitions, and some key results concerning nonlinear nonnegative dynamical systems that are necessary for developing the main results of this paper. Specifically, for $x \in \mathbb{R}^n$ we write $x \geq\geq 0$ (resp., $x >> 0$) to indicate that every component of x is nonnegative (resp., positive). In this case, we say that x is *nonnegative* or *positive*, respectively. Likewise, $A \in \mathbb{R}^{n\times m}$ is *nonnegative* or *positive* if every entry of A is nonnegative or positive, respectively, which is written as $A \geq\geq 0$ or $A >> 0$, respectively. Let $\overline{\mathbb{R}}_+^n$ and $\mathbb{R}_+^n$ denote the nonnegative and positive orthants of $\mathbb{R}^n$, that is, if $x \in \mathbb{R}^n$, then $x \in \overline{\mathbb{R}}_+^n$ and $x \in \mathbb{R}_+^n$ are equivalent, respectively, to $x \geq\geq 0$ and $x >> 0$. Furthermore, we write $(\cdot)^{\mathrm{T}}$ to denote transpose, $\mathrm{tr}(\cdot)$ for the trace operator, $\lambda_{\min}(\cdot)$ to denote the minimum eigenvalue of a Hermitian matrix, and $\|\cdot\|$ for a vector norm. Finally, $M \otimes N$ denotes the Kronecker product of matrices M and N. The following definition introduces the notion of a nonnegative (resp., positive) function.

Definition 2.1: Let $T > 0$. A real function $u : [0, T] \to \mathbb{R}^m$ is a *nonnegative* (resp., *positive*) *function* if $u(t) \geq\geq 0$ (resp., $u(t) >> 0$) on the interval $[0, T]$.

The following definition introduces the notion of essentially nonnegative vector fields.

Definition 2.2: Let $f = [f_1, \cdots, f_n]^{\mathrm{T}} : \mathcal{D} \to \mathbb{R}^n$, where $\mathcal{D}$ is an open subset of $\mathbb{R}^n$ that contains $\overline{\mathbb{R}}_+^n$. Then f is *essentially nonnegative* if $f_i(x) \geq 0$, for all $i = 1, \ldots, n$, and $x \in \overline{\mathbb{R}}_+^n$ such that $x_i = 0$, where x_i denotes the ith element of x.

In this paper, we consider controlled nonlinear dynamical systems of the form

$$\dot{x}(t) = f(x(t)) + G(x(t))u(t),\ x(0) = x_0,\ t \geq 0, \qquad (1)$$

where $x(t) \in \mathbb{R}^n$, $t \geq 0$, $u(t) \in \mathbb{R}^m$, $t \geq 0$, $f : \mathbb{R}^n \to \mathbb{R}^n$ is locally Lipschitz continuous and satisfies $f(0) = 0$, $G : \mathbb{R}^n \to \mathbb{R}^{n\times m}$ is continuous, and $u : [0, \infty) \to \mathbb{R}^m$ is piecewise continuous.

The following definition is needed.

Definition 2.3: The nonlinear dynamical system given by (1) is *nonnegative* if for every $x(0) \in \overline{\mathbb{R}}_+^n$ and $u(t) \geq\geq 0$, $t \geq 0$, the solution $x(t)$, $t \geq 0$, to (1) is nonnegative.

III. Neuroadaptive Output Feedback Control for Nonlinear Nonnegative Uncertain Systems

In this section, we consider the problem of characterizing neuroadaptive dynamic output feedback control laws for nonlinear nonnegative and compartmental uncertain dynamical systems to achieve *set-point* regulation in the nonnegative orthant. Specifically, consider the controlled square nonlinear uncertain dynamical system $\mathcal{G}$ given by

$$\dot{x}(t) = f(x(t)) + G(x(t))u(t),\ x(0) = x_0,\ t \geq 0, \qquad (2)$$
$$y(t) = h(x(t)), \qquad (3)$$
$$y_{\mathrm{n}}(t) = y(t) + n(t), \qquad (4)$$

where $x(t) \in \mathbb{R}^n$, $t \geq 0$, is the state vector, $u(t) \in \mathbb{R}^m$, $t \geq 0$, is the control input, $y(t) \in \mathbb{R}^m$, $t \geq 0$, is the system output, $y_{\mathrm{n}}(t) \in \mathbb{R}^m$, $t \geq 0$, is the noisy system output, $n(t) \in \mathbb{R}^m$, $t \geq 0$, is a noise signal such that $\|n(t)\| \leq n^* < \infty$ for all $t \geq 0$, $f : \mathbb{R}^n \to \mathbb{R}^n$, is essentially nonnegative but otherwise unknown, $G : \mathbb{R}^n \to \mathbb{R}^{n\times m}$ is an unknown nonnegative input matrix function, and $h : \mathbb{R}^n \to \mathbb{R}^m$ is a nonnegative output function. We assume that $f(\cdot)$, $G(\cdot)$, and $h(\cdot)$ are smooth (at least C^n mappings) and the control input $u(\cdot)$ in (2) is restricted to the class of *admissible controls* consisting of measurable functions such that $u(t) \in \mathbb{R}^m$, $t \geq 0$.

As discussed in [6]–[8], control (source) inputs of drug delivery systems for physiological and pharmacological processes are usually constrained to be nonnegative as are the system states. Hence, in this paper we develop neuroadaptive dynamic output feedback control laws for nonnegative systems with nonnegative control inputs. Specifically, for a given desired set point $y_{\mathrm{d}} \in \overline{\mathbb{R}}_+^m$ and for a given $\varepsilon > 0$, our aim is to design a nonnegative control input $u(t)$, $t \geq 0$, predicated on the system measurement $y_{\mathrm{n}}(t)$, $t \geq 0$, such that $\|y(t) - y_{\mathrm{d}}\| < \varepsilon$ for all $t \geq T$, where $T \in [0, \infty)$, and $x(t) \geq\geq 0$, $t \geq 0$, for all $x_0 \in \overline{\mathbb{R}}_+^n$.

In this paper, we assume that for the nonlinear dynamical system (2) and (3), the conditions for the existence of a globally defined diffeomorphism transforming (2) and (3) into a normal form are satisfied. Specifically, we assume that there exist a global diffeomorphism $\mathcal{T} : \mathbb{R}^n \to \mathbb{R}^n$ and C^n functions $f_\xi : \mathbb{R}^r \times \mathbb{R}^{n-r} \to \mathbb{R}^r$ and $f_z : \mathbb{R}^r \times \mathbb{R}^{n-r} \to \mathbb{R}^{n-r}$ such that, in the coordinates $\left[\xi^{\mathrm{T}},\ z^{\mathrm{T}}\right]^{\mathrm{T}} \triangleq \mathcal{T}(x)$, where $\xi \triangleq [y_1, \dot{y}_1, \cdots, y_1^{(r_1-2)}, \cdots, y_m, \dot{y}_m, \cdots, y_m^{(r_m-2)}; y_1^{(r_1-1)}, \cdots, y_m^{(r_m-1)}] \in \mathbb{R}^r$, $y_i^{(r_i)}$ denotes the r_ith derivative of y_i, r_i denotes the relative degree of $\mathcal{G}$ with respect to the output y_i, $z \in \mathbb{R}^{n-r}$, and $r \triangleq r_1 + \cdots + r_m$ is the (vector) relative degree of $\mathcal{G}$, the nonlinear dynamical system $\mathcal{G}$ given by (2)–(4) is equivalent to

$$\begin{aligned}
\dot{\xi}(t) &= f_\xi(\xi(t), z(t)) + G_\xi(\xi(t), z(t))u(t), \\
&\qquad \xi(0) = \xi_0, \quad t \geq 0, \qquad (5)\\
\dot{z}(t) &= f_z(\xi(t), z(t)), \quad z(0) = z_0, \qquad (6)\\
y(t) &= C\xi(t), \qquad (7)\\
y_{\mathrm{n}}(t) &= C\xi(t) + n(t), \qquad (8)
\end{aligned}$$

where $\xi(t) \in \mathbb{R}^r$, $t \geq 0$, $z(t) \in \mathbb{R}^{n-r}$, $t \geq 0$,

$$f_\xi(\xi, z) = A\xi + \tilde{f}_{\mathrm{u}}(\xi, z),\ G_\xi(\xi, z) = \left[\begin{array}{c} 0_{(r-m)\times m} \\ \hat{G}(\tilde{x}) \end{array} \right], \quad (9)$$

$$A = \left[\begin{array}{c} A_0 \\ \hat{A} \end{array} \right], \quad \tilde{f}_{\mathrm{u}}(\xi, z) = \left[\begin{array}{c} 0_{(r-m)\times 1} \\ f_{\mathrm{u}}(\tilde{x}) \end{array} \right], \quad (10)$$

$\tilde{x} \triangleq [\xi^{\mathrm{T}}, z^{\mathrm{T}}]^{\mathrm{T}}$, $A_0 \in \mathbb{R}^{(r-m)\times r}$ is a known matrix of zeros and ones capturing the multivariable controllable canonical form representation, $\hat{A} \in \mathbb{R}^{m\times r}$ is such that A is asymptotically stable, $f_{\mathrm{u}} : \mathbb{R}^n \to \mathbb{R}^m$ is an unknown function, $C \in \mathbb{R}^{m\times r}$ is a known matrix of zeros and ones capturing the system output, and $\hat{G} : \mathbb{R}^n \to \mathbb{R}^{m\times m}$ is an unknown matrix function such that $\det \hat{G}(\tilde{x}) \neq 0$, $\tilde{x} \in \mathbb{R}^n$. Furthermore, we assume that for a given $y_{\mathrm{d}} \in \overline{\mathbb{R}}_+^m$ there exist $z_{\mathrm{e}} \in \mathbb{R}^{n-r}$ and $u_{\mathrm{e}} \in \overline{\mathbb{R}}_+^m$ such that $x_{\mathrm{e}} \triangleq \mathcal{T}^{-1}(\tilde{x}_{\mathrm{e}}) \geq\geq 0$ and

$$0 = f_\xi(\xi_{\mathrm{e}}, z_{\mathrm{e}}) + G_\xi(\xi_{\mathrm{e}}, z_{\mathrm{e}})u_{\mathrm{e}}, \quad (11)$$

$$0 = f_z(\xi_{\mathrm{e}}, z_{\mathrm{e}}), \quad (12)$$

where $\tilde{x}_{\mathrm{e}} \triangleq [\xi_{\mathrm{e}}^{\mathrm{T}}, z_{\mathrm{e}}^{\mathrm{T}}]^{\mathrm{T}}$ and ξ_{e} is given with $y_i = y_{\mathrm{d}i}$, $i = 1, \ldots, m$, and $\dot{y}_i = \cdots = y_i^{(r_i-1)} = 0$, $i = 1, \ldots, m$.

To ensure that for a bounded state $\xi(t)$, $t \geq 0$, the dynamics given by (6) are bounded, we assume that (6) is input-to-state stable at $z(t) \equiv z_{\mathrm{e}}$ with $\xi(t) - \xi_{\mathrm{e}}$ viewed as the input; that is, there exist a class $\mathcal{KL}$ function $\eta(\cdot, \cdot)$ and a class $\mathcal{K}$ function $\gamma(\cdot)$ such that, for $t \geq 0$,

$$\|z(t) - z_{\mathrm{e}}\| \leq \eta(\|z_0 - z_{\mathrm{e}}\|, t) + \gamma\left(\sup_{0\leq\tau\leq t} \|\xi(\tau) - \xi_{\mathrm{e}}\| \right),$$

where $\|\cdot\|$ denotes the Euclidean vector norm. Unless otherwise stated, henceforth we use $\|\cdot\|$ to denote the Euclidean vector norm. Note that $(\xi_{\mathrm{e}}, z_{\mathrm{e}}) \in \mathbb{R}^r \times \mathbb{R}^{n-r}$ is an equilibrium point of (5) and (6) if and only if there exists $u_{\mathrm{e}} \in \overline{\mathbb{R}}_+^m$ such that (11) and (12) hold.

Finally, we assume that the functions $f_{\mathrm{u}}(\mathcal{T}(x)) - f_{\mathrm{u}}(\mathcal{T}(x_{\mathrm{e}})) - \hat{G}(\mathcal{T}(x_{\mathrm{e}}))u_{\mathrm{e}}$ and $\hat{G}(\mathcal{T}(x)) - \hat{B}$, where $\hat{B} \in \mathbb{R}^{m\times m}$, can be approximated over a compact set $\mathcal{D}_{\mathrm{c}} \subset \overline{\mathbb{R}}_+^n$ by a linear in the parameters neural network up to a desired accuracy. In this case, there exist $\varepsilon_1 : \mathbb{R}^n \to \mathbb{R}^m$ and $\varepsilon_2 : \mathbb{R}^n \to \mathbb{R}^{m\times m}$ such that $\|\varepsilon_1(x)\| < \varepsilon_1^*$ and $\|\varepsilon_2(x)\|_{\mathrm{F}} < \varepsilon_2^*$, $x \in \mathcal{D}_{\mathrm{c}}$, where $\varepsilon_1^* > 0$ and $\varepsilon_2^* > 0$, and

$$f_{\mathrm{u}}(\mathcal{T}(x)) - f_{\mathrm{u}}(\mathcal{T}(x_{\mathrm{e}})) - \hat{G}(\mathcal{T}(x_{\mathrm{e}}))u_{\mathrm{e}} = W_1^{\mathrm{T}}\hat{\sigma}_1(x) + \varepsilon_1(x), \quad (13)$$

$$\hat{G}(\mathcal{T}(x)) - \hat{B} = W_2^{\mathrm{T}}[I_m \otimes \hat{\sigma}_2(x)] + \varepsilon_2(x), \quad (14)$$

where $x \in \mathcal{D}_{\mathrm{c}}$, $W_1 \in \mathbb{R}^{s_1\times m}$ and $W_2 \in \mathbb{R}^{ms_2\times m}$ are optimal *unknown* (constant) weights that minimize the approximation errors over $\mathcal{D}_{\mathrm{c}}$, $\hat{\sigma}_1 : \mathbb{R}^n \to \mathbb{R}^{s_1}$ and $\hat{\sigma}_2 : \mathbb{R}^n \to \mathbb{R}^{s_2}$ are sets of basis functions such that each component of $\hat{\sigma}_1(\cdot)$ and $\hat{\sigma}_2(\cdot)$ takes values between 0 and 1, and $\varepsilon_1(\cdot)$ and $\varepsilon_2(\cdot)$ are the modeling errors. Note that $s_1 + s_2$ denotes the total number of basis functions or, equivalently, the number of nodes of the neural network.

Since $f_{\mathrm{u}}(\cdot)$ and $\hat{G}(\cdot)$ are continuous, we can choose $\hat{\sigma}_1(\cdot)$ and $\hat{\sigma}_2(\cdot)$ from a linear space $\mathcal{X}$ of continuous functions that forms an algebra and separates points in $\mathcal{D}_{\mathrm{c}}$. In this case, it follows from the Stone-Weierstrass theorem that $\mathcal{X}$ is a dense subset of the set of continuous functions on $\mathcal{D}_{\mathrm{c}}$. Now, as is the case in the standard neuroadaptive control literature, we can construct the signal $u_{\mathrm{ad}} = F(\hat{W}_1, \hat{W}_2, \hat{\sigma}_1(x), \hat{\sigma}_2(x))$, where $F : \mathbb{R}^{s_1\times m} \times \mathbb{R}^{ms_2\times m} \times \mathbb{R}^{s_1} \times \mathbb{R}^{s_2} \to \mathbb{R}^m$, involving the estimates of the optimal weights and basis functions as our adaptive control signal.

Since the actual measurement $y_{\mathrm{n}}(t)$, $t \geq 0$, is noisy with $n(t)$, $t \geq 0$, representing a high-frequency noise signal, we use a filtered version of $y_{\mathrm{n}}(t)$, $t \geq 0$, in the control input $u(t)$, $t \geq 0$. Specifically, we design an asymptotically stable low-pass filter of the form

$$\dot{x}_{\mathrm{f}}(t) = A_{\mathrm{f}}x_{\mathrm{f}}(t) + B_{\mathrm{f}}y_{\mathrm{n}}(t), \quad x_{\mathrm{f}}(0) = x_{\mathrm{f}_0}, \quad t \geq 0, \quad (15)$$

$$y_{\mathrm{f}}(t) = C_{\mathrm{f}}x_{\mathrm{f}}(t), \quad (16)$$

where $A_{\mathrm{f}} \in \mathbb{R}^{n_{\mathrm{f}}\times n_{\mathrm{f}}}$ is Hurwitz and essentially nonnegative and $B_{\mathrm{f}} \in \mathbb{R}^{n_{\mathrm{f}}\times m}$ and $C_{\mathrm{f}} \in \mathbb{R}^{m\times n_{\mathrm{f}}}$ are nonnegative matrices such that $\lim_{\omega\to\infty} |G_{(i,j)}(j\omega)| = 0$, $i, j = 1, \ldots, m$, where $G_{(i,j)}(s)$ denotes the (i, j)th entry of the transfer function $G(s) \triangleq C_{\mathrm{f}}(sI_{n_{\mathrm{f}}} - A_{\mathrm{f}})^{-1}B_{\mathrm{f}}$. Here, we choose the matrices A_{f}, B_{f}, and C_{f} such that $C_{\mathrm{f}}A_{\mathrm{f}}^{-1}B_{\mathrm{f}} = -I_m$. In this case, for every $y_{\mathrm{d}} \in \overline{\mathbb{R}}_+^m$, there exists $x_{\mathrm{f}_{\mathrm{e}}} \in \mathbb{R}^{n_{\mathrm{f}}}$ such that

$$0 = A_{\mathrm{f}}x_{\mathrm{f}_{\mathrm{e}}} + B_{\mathrm{f}}y_{\mathrm{d}}, \quad (17)$$

$$y_{\mathrm{d}} = C_{\mathrm{f}}x_{\mathrm{f}_{\mathrm{e}}}. \quad (18)$$

Note that since A_{f} is Hurwitz there exist positive-definite matrices $\hat{P} \in \mathbb{R}^{n_{\mathrm{f}}\times n_{\mathrm{f}}}$ and $\hat{R} \in \mathbb{R}^{n_{\mathrm{f}}\times n_{\mathrm{f}}}$ such that

$$0 = A_{\mathrm{f}}^{\mathrm{T}}\hat{P} + \hat{P}A_{\mathrm{f}} + \hat{R}. \quad (19)$$

In order to develop an *output* feedback neural network, we use the recent approach developed in [10] for reconstructing the system states via the system delayed inputs and filtered outputs. Specifically, we use a *memory unit* as a particular form of a tapped delay line that takes a scalar time series input and provides an $(2mn - r)$-dimensional vector output consisting of the present values of the system filtered outputs and system inputs, and their $2(n-1)m - r$ delayed values given by

$$\begin{aligned}\zeta(t) \triangleq [&y_{\mathrm{f}_1}(t), y_{\mathrm{f}_1}(t-d), \ldots, y_{\mathrm{f}_1}(t-(n-1)d), \ldots,\\ &y_{\mathrm{f}_m}(t), y_{\mathrm{f}_m}(t-d), \ldots, y_{\mathrm{f}_m}(t-(n-1)d);\\ &u_1(t), u_1(t-d), \ldots, u_1(t-(n-r_1-1)d), \ldots,\\ &u_m(t), u_m(t-d), \ldots, u_m(t-(n-r_m-1)d)]^{\mathrm{T}},\\ &t \geq 0, \quad (20)\end{aligned}$$

where $d > 0$.

For the statement of our main result, define the projection operator $\mathrm{Proj}(\tilde{W}, Y)$ given by

$$\mathrm{Proj}(\tilde{W}, Y) \triangleq \begin{cases} Y, & \text{if } \mu(\tilde{W}) < 0,\\ Y, & \text{if } \mu(\tilde{W}) \geq 0 \text{ and } \mu'(\tilde{W})Y \leq 0,\\ Y - \frac{\mu' T(\tilde{W})\mu'(\tilde{W})Y}{\mu'(\tilde{W})\mu' T(\tilde{W})}\mu(\tilde{W}), & \text{otherwise,} \end{cases}$$

where $\tilde{W} \in \mathbb{R}^{s\times m}$, $Y \in \mathbb{R}^{n\times m}$, $\mu(\tilde{W}) \triangleq \frac{\mathrm{tr}\,\tilde{W}^{\mathrm{T}}\tilde{W} - \tilde{w}_{\max}^2}{\varepsilon_{\tilde{W}}}$, $\tilde{w}_{\max} \in \mathbb{R}$ is the norm bound imposed on $\tilde{W}$, and $\varepsilon_{\tilde{W}} > 0$. Note that for a given matrix $\tilde{W} \in \mathbb{R}^{s\times m}$ and $Y \in \mathbb{R}^{n\times m}$, it follows that

$$\begin{aligned}&\mathrm{tr}[(\tilde{W} - W)^{\mathrm{T}}(\mathrm{Proj}(\tilde{W}, Y) - Y)]\\ &= \sum_{i=1}^{n}[\mathrm{col}_i(\tilde{W} - W)]^{\mathrm{T}}[\mathrm{Proj}(\mathrm{col}_i(\tilde{W}), \mathrm{col}_i(Y)) - \mathrm{col}_i(Y)]\\ &\leq 0, \quad (21)\end{aligned}$$

where $\mathrm{col}_i(X)$ denotes the ith column of the matrix X.

Assumption 4.1. For a given $y_{\rm d} \in \overline{\mathbb{R}}_+^m$ assume there exist nonnegative vectors $x_{\rm e} \in \overline{\mathbb{R}}_+^n$ and $u_{\rm e} \in \overline{\mathbb{R}}_+^m$ such that

$$0 = f(x_{\rm e}) + G(x_{\rm e})u_{\rm e}, \tag{22}$$

$$y_{\rm d} = h(x_{\rm e}). \tag{23}$$

Furthermore, assume that the equilibrium point $x_{\rm e}$ of (2) is globally asymptotically stable with $u(t) \equiv u_{\rm e}$. Finally, assume that there exists a global diffeomorphism $\mathcal{T} : \mathbb{R}^n \to \mathbb{R}^n$ such that $\mathcal{G}$ can be transformed into the normal form given by (5) and (6), and (6) is input-to-state stable at $z_{\rm e}$ with $\xi(t) - \xi_{\rm e}$ viewed as the input.

Consider the neuroadaptive output feedback control law given by

$$u(t) = \begin{cases} \hat{u}(t), & \text{if } \hat{u}(t) \geq\geq 0, \\ 0, & \text{otherwise,} \end{cases} \tag{24}$$

where

$$\hat{u}(t) = -\left(\hat{B} + \hat{W}_2^{\rm T}(t)[I_m \otimes \sigma_2(\zeta(t))]\right)^{-1} \hat{W}_1^{\rm T}(t)\sigma_1(\zeta(t)), \tag{25}$$

$\hat{B} \in \mathbb{R}^{m\times m}$ is nonsingular, $\zeta(t)$, $t \geq 0$, is given by (20), $\sigma_1 : \mathbb{R}^n \to \mathbb{R}^{s_1}$ and $\sigma_2 : \mathbb{R}^n \to \mathbb{R}^{s_2}$ are sets of basis functions such that each component of $\sigma_1(\cdot)$ and $\sigma_2(\cdot)$ takes values between 0 and 1, $\hat{W}_1(t) \in \mathbb{R}^{s_1\times m}$, $t \geq 0$, and $\hat{W}_2(t) \in \mathbb{R}^{ms_2\times m}$, $t \geq 0$. Here, the update laws satisfy

$$\dot{\hat{W}}_1(t) = Q_1 \mathrm{Proj}[\hat{W}_1(t), -\sigma_1(\zeta(t))\xi_{\rm c}^{\rm T}(t)\tilde{P}B_0], \quad \hat{W}_1(0) = \hat{W}_{10}, \quad t \geq 0, \tag{26}$$

$$\dot{\hat{W}}_2(t) = Q_2 \mathrm{Proj}[\hat{W}_2(t), -[I_m \otimes \sigma_2(\zeta(t))]u(t)\xi_{\rm c}^{\rm T}(t)\tilde{P}B_0], \quad \hat{W}_2(0) = \hat{W}_{20}, \quad t \geq 0, \tag{27}$$

where $Q_1 \in \mathbb{R}^{s_1\times s_1}$ and $Q_2 \in \mathbb{R}^{ms_2\times ms_2}$ are positive definite matrices, $\tilde{P} \in \mathbb{R}^{r\times r}$ is a positive-definite solution of the Lyapunov equation

$$0 = (A - LC)^{\rm T}\tilde{P} + \tilde{P}(A - LC) + \tilde{R}, \tag{28}$$

where $\tilde{R} > 0$, and $\xi_{\rm c}(t)$, $t \geq 0$, is the solution to the estimator dynamics

$$\dot{\xi}_{\rm c}(t) = A\xi_{\rm c}(t) + L(y_{\rm f}(t) - y_{\rm c}(t) - y_{\rm d}), \quad \xi_{\rm c}(0) = \xi_{\rm c0}, \quad t \geq 0, \tag{29}$$

$$y_{\rm c}(t) = C\xi_{\rm c}(t), \tag{30}$$

where $\xi_{\rm c}(t) \in \mathbb{R}^r$, $t \geq 0$, $A \in \mathbb{R}^{r\times r}$ is given by (10), $L \in \mathbb{R}^{r\times m}$ is such that $A - LC$ is Hurwitz, $y_{\rm f}(t)$, $t \geq 0$, is the output of the filter (15) and (16), and $B_0 \triangleq [0_{m\times(r-m)}, I_m]^{\rm T}$.

Theorem 3.1: Consider the nonlinear uncertain dynamical system $\mathcal{G}$ given by (2) and (3) with $u(t)$, $t \geq 0$, given by (24). Assume Assumption 4.1 holds, $\lambda_{\min}(RP^{-1}) > 1$, and $\lambda_{\min}(\hat{R}) > \|\hat{P}B_{\rm f}CP^{-1/2}\|$, where $\hat{P} \in \mathbb{R}^{n_{\rm f}\times n_{\rm f}}$ and $P \in \mathbb{R}^{r\times r}$ are the positive-definite solutions of the Lyapunov equations (19) and

$$0 = A^{\rm T}P + PA + R, \tag{31}$$

where $R > 0$. Then there exists a compact positively invariant set $\mathcal{D}_\alpha \subset \mathbb{R}^n \times \mathbb{R}^r \times \mathbb{R}^{s_1\times m} \times \mathbb{R}^{ms_2\times m} \times \mathbb{R}^{n_{\rm f}}$ such that $(x_{\rm e}, 0, W_1, W_2, x_{\rm f_e}) \in \mathcal{D}_\alpha$, where $W_1 \in \mathbb{R}^{s_1\times m}$ and $W_2 \in \mathbb{R}^{ms_2\times m}$, and the solution $(x(t), \xi_{\rm c}(t), \hat{W}_1(t), \hat{W}_2(t), x_{\rm f}(t))$, $t \geq 0$, of the closed-loop system given by (2), (15), (16), (24), (26), (27), (29), and (30) is ultimately bounded for all $(x(0), \xi_{\rm c}(0), \hat{W}_1(0), \hat{W}_2(0), x_{\rm f}(0)) \in \mathcal{D}_\alpha$. Furthermore, $u(t) \geq\geq 0$, $t \geq 0$, and $x(t) \geq\geq 0$, $t \geq 0$, for all $x_0 \in \overline{\mathbb{R}}_+^n$.

Since the norm of $\hat{W}_2(t)$ is bounded it is always possible to choose $\hat{B}$ so that $(\hat{B}+\hat{W}_2^{\rm T}(t)[I_m\otimes\sigma_2(\zeta(t))])^{-1}$ exists and is bounded for all $t \geq 0$ so that there exists $u^* > 0$ such that $u^* \geq \|u(t)\|$, $t \geq 0$. Implementing the neuroadaptive controller (25) requires a fixed-point iteration at each integration step, that is, the controller contains an algebraic constraint on u. For each choice of $\sigma_1(\cdot)$ and $\sigma_2(\cdot)$ this equation must be examined for solvability in terms of u. It is more practical to avoid this iteration by using one-step delayed values of u in calculating $\hat{u}$. Implementations using both approaches result in imperceptible differences in our numerical studies.

IV. Neuroadaptive Output Feedback Control for General Anesthesia

To illustrate the application of the neuroadaptive control framework presented in Section III for general anesthesia we develop a model for the intravenous anesthetic propofol. The pharmacokinetics of propofol are described by the three compartment model shown in Figure 1, where x_1 denotes the mass of drug in the central compartment, which is the site for drug administration and is generally thought to be comprised of the *intravascular blood* volume (blood within arteries and veins) as well as *highly perfused* organs (organs with high ratios of blood flow to weight) such as the heart, brain, kidney, and liver. These organs receive a large fraction of the cardiac output. The remainder of the drug in the body is assumed to reside in two peripheral compartments, one identified with muscle and one with fat; the masses in these compartments are denoted by x_2 and x_3, respectively. These compartments receive less than 20% of the cardiac output.

A mass balance of the three-state compartmental model yields

$$\dot{x}_1(t) = -[a_{11}(c(t)) + a_{21}(c(t)) + a_{31}(c(t))]x_1(t) + a_{12}(c(t))x_2(t) + a_{13}(c(t))x_3(t) + u(t), \quad x_1(0) = x_{10}, \quad t \geq 0, \tag{32}$$

$$\dot{x}_2(t) = a_{21}(c(t))x_1(t) - a_{12}(c(t))x_2(t), \quad x_2(0) = x_{20}, \quad t \geq 0, \tag{33}$$

$$\dot{x}_3(t) = a_{31}(c(t))x_1(t) - a_{13}(c(t))x_3(t), \quad x_3(0) = x_{30}, \quad t \geq 0, \tag{34}$$

where $c(t) = x_1(t)/V_{\rm c}$, $V_{\rm c}$ is the volume of the central compartment (about 15 l for a 70 kg patient), $a_{ij}(c)$, $i \neq j$, is the rate of transfer of drug from the jth compartment to the ith compartment, $a_{11}(c)$ is the rate of drug metabolism and elimination (metabolism typically occurs in the liver), and $u(t)$, $t \geq 0$, is the infusion rate of the anesthetic drug propofol into the central compartment. The transfer coefficients are assumed to be functions of the drug concentration c since it is well known that the pharmacokinetics of propofol are influenced by cardiac output [11] and, in turn, cardiac output is influenced by propofol plasma concentrations, both due to *venodilation* (pooling of blood in dilated vains) [12] and myocardial depression [13].

Experimental data indicate that the transfer coefficients $a_{ij}(\cdot)$ are nonincreasing functions of the propofol concentration [12], [13]. The most widely used empirical models for pharmacodynamic concentration-effect relationships are modifications of the Hill equation. Applying this almost ubiquitous empirical model to the relationship between transfer coefficients implies that

$$a_{ij}(c) = A_{ij}Q_{ij}(c), \quad Q_{ij}(c) = Q_0{\rm C}_{50,ij}^{\alpha_{ij}}/({\rm C}_{50,ij}^{\alpha_{ij}} + c^{\alpha_{ij}}),$$

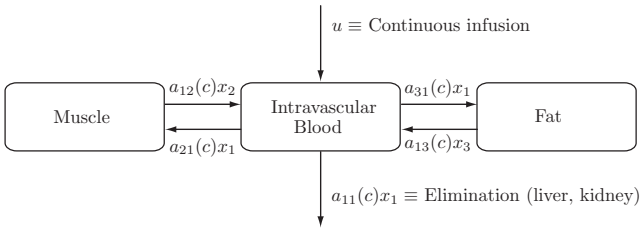

Fig. 1. Pharmacokinetic model for drug distribution during anesthesia

where, for $i, j \in \{1, 2, 3\}$, $i \neq j$, $\mathrm{C}_{50,ij}$ is the drug concentration associated with a 50% decrease in the transfer coefficient, α_{ij} is a parameter that determines the steepness of the concentration-effect relationship, and A_{ij} are positive constants. Note that both pharmacokinetic parameters are functions of i and j, that is, there are distinct Hill equations for each transfer coefficient. Furthermore, since for many drugs the rate of metabolism $a_{11}(c)$ is proportional to the rate of transport of drug to the liver we assume that $a_{11}(c)$ is also proportional to the cardiac output so that $a_{11}(c) = A_{11}Q_{11}(c)$.

To illustrate the neuroadaptive control of propofol, we assume that $\mathrm{C}_{50,ij}$ and α_{ij} are independent of i and j. Also, since decreases in cardiac output are observed at clinically-utilized propofol concentrations we arbitrarily assign C_{50} a value of 4 μg/ml since this value is in the mid-range of clinically utilized values. We also assign α a value of 3. This value is within the typical range of those observed for ligand-receptor binding. The nonnegative transfer and loss coefficients A_{12}, A_{21}, A_{13}, A_{31}, and A_{11}, and the parameters $\alpha > 1$, $\mathrm{C}_{50} > 0$, and $Q_0 > 0$, are uncertain due to patient gender, weight, pre-existing disease, age, and concomitant medication. Hence, the need for adaptive control to regulate intravenous anesthetics during surgery is essential.

Even though propofol concentration levels in the blood plasma will lead to the desired depth of anesthesia, they cannot be measured in real-time during surgery. Furthermore, we are more interested in drug *effect* (depth of hypnosis) rather than drug *concentration*. Hence, we consider a model involving pharmacokinetics (drug concentration as a function of time) and pharmacodynamics (drug effect as a function of concentration) for controlling consciousness. Specifically, we use an electroencephalogram (EEG) signal as a measure of hypnotic drug effect of anesthetic compounds on the brain [3]. Since electroencephalography provides real-time monitoring of the central nervous system activity, it can be used to quantify levels of consciousness, and hence, is amenable for feedback control in general anesthesia.

The Bispectral Index (BIS), an EEG indicator, has been proposed as a measure of hypnotic effect. This index quantifies the nonlinear relationships between the component frequencies in the electroencephalogram, as well as analyzing their phase and amplitude. The BIS signal is related to drug concentration by the empirical relationship

$$\mathrm{BIS}_{\mathrm{n}}(c_{\mathrm{eff}}(t)) = \mathrm{BIS}_0 \left(1 - \frac{c_{\mathrm{eff}}^{\gamma}(t)}{c_{\mathrm{eff}}^{\gamma}(t) + \mathrm{EC}_{50}^{\gamma}}\right) + n(t), \quad (35)$$

where BIS_0 denotes the baseline (awake state) value and, by convention, is typically assigned a value of 100, c_{eff} is the propofol concentration in μg/ml in the effect-site compartment (brain), EC_{50} is the concentration at half maximal effect and represents the patient's sensitivity to the drug, γ determines the degree of nonlinearity in (35), and n is a high-frequency observation noise signal. Here, the effect-site compartment is introduced to account for finite equilibration time between the central compartment concentration and the central nervous system concentration.

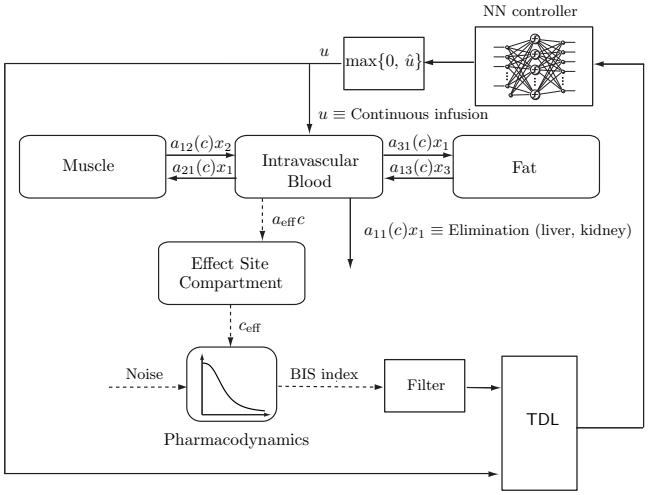

Fig. 2. Combined pharmacokinetic/pharmacodynamic model

The effect-site compartment concentration is related to the concentration in the central compartment by the first-order model

$$\dot{c}_{\mathrm{eff}}(t) = a_{\mathrm{eff}}(c(t) - c_{\mathrm{eff}}(t)), \quad c_{\mathrm{eff}}(0) = c(0), \quad t \geq 0, \quad (36)$$

where a_{eff} in min^{-1} is an unknown positive time constant. In reality, the effect-site compartment equilibrates with the central compartment in a matter of a few minutes. The parameters a_{eff}, EC_{50}, and γ are determined by data fitting and vary from patient to patient. BIS index values of 0 and 100 correspond, respectively, to an *isoelectric* EEG signal (no cerebral electrical activity) and an EEG signal of a fully conscious patient; the range between 40 and 60 indicates a moderate hypnotic state. Figure 2 shows the combined pharmacokinetic/pharmacodynamic feedback control model for the distribution of propofol.

In the following simulation involving the infusion of the anesthetic drug propofol we set $\mathrm{EC}_{50} = 5.6$ μg/ml, $\gamma = 2.39$, and $\mathrm{BIS}_0 = 100$. The target (desired) BIS value, $\mathrm{BIS}_{\mathrm{target}}$, is set at 50. Here, we use the neuroadaptive output feedback controller $u(t) = \max\{0, \hat{u}(t)\}$, where

$$\hat{u}(t) = -\frac{\hat{W}_1^{\mathrm{T}}(t)\sigma_1(\zeta(t))}{\hat{b} + \hat{W}_2^{\mathrm{T}}(t)\sigma_2(\zeta(t))},$$

$$\zeta(t) = [\mathrm{BIS}_{\mathrm{f}}(t-d), \mathrm{BIS}_{\mathrm{f}}(t-2d), u(t-d), u(t-2d)]^{\mathrm{T}},$$

$\hat{b} > 0$, $d > 0$, with update laws

$$\begin{aligned} \dot{\hat{W}}_1(t) &= Q_{\mathrm{BIS}_1}\mathrm{Proj}[\hat{W}_1(t), -\sigma_1(\zeta(t))\xi_{\mathrm{c}}^{\mathrm{T}}(t)\tilde{P}B_0], \\ \dot{\hat{W}}_2(t) &= Q_{\mathrm{BIS}_2}\mathrm{Proj}[\hat{W}_2(t), -\sigma_2(\zeta(t))u(t)\xi_{\mathrm{c}}^{\mathrm{T}}(t)\tilde{P}B_0], \\ & \quad \hat{W}_1(0) = \hat{W}_{10}, \quad \hat{W}_2(0) = \hat{W}_{20}, \quad t \geq 0, \end{aligned}$$

where Q_{BIS_1} and Q_{BIS_2} are positive constants and $\xi_{\mathrm{c}}(t) \in \mathbb{R}^2$, $t \geq 0$, is the solution to the estimator dynamics

$$\dot{\xi}_{\mathrm{c}}(t) = A\xi_{\mathrm{c}}(t) + L(-\mathrm{BIS}_{\mathrm{f}}(t) - y_{\mathrm{c}}(t) + \mathrm{BIS}_{\mathrm{target}}), \quad (37)$$

$$y_{\mathrm{c}}(t) = \xi_{\mathrm{c}}(t), \quad \xi_{\mathrm{c}}(0) = \xi_{\mathrm{c}0}, \quad t \geq 0, \quad (38)$$

where $A \in \mathbb{R}^{2\times 2}$ and $L \in \mathbb{R}^{2\times 1}$, and $\mathrm{BIS}_{\mathrm{f}}(t)$ is output of the second-order, low-pass stable filter

$$\begin{aligned} \dot{x}_{\mathrm{f}}(t) &= A_{\mathrm{f}}x_{\mathrm{f}}(t) + B_{\mathrm{f}}\mathrm{BIS}_{\mathrm{n}}(t), \quad t \geq 0 \quad (39) \\ \mathrm{BIS}_{\mathrm{f}}(t) &= C_{\mathrm{f}}x_{\mathrm{f}}(t), \quad x_{\mathrm{f}}(0) = [\mathrm{BIS}_{\mathrm{f}}(0), 0]^{\mathrm{T}}, \quad (40) \end{aligned}$$

where $A_{\rm f} = \begin{bmatrix} 0 & 1 \\ -\omega^2 & -2\zeta\omega \end{bmatrix}$, $B_{\rm f} = [0,\ \omega^2]^{\rm T}$, $C_{\rm f} = [1, 0]^{\rm T}$, $\omega = 5$ rad/sec, $\zeta = 0.7$, and $\mathrm{BIS_f}(0) = 100$. Here, we model $n(t)$ as a noise signal generated by a SIMULINK band-limited white noise block with noise power parameter equal 0.0001 amplified 100 times. Now, it follows from Theorem 3.1 that there exist positive constants ε and T such that $|\mathrm{BIS}(t) - \mathrm{BIS_{target}}| \leq \varepsilon$, $t \geq T$, where $\mathrm{BIS}(t)$ is given by (35) with $n(t) \equiv 0$, for all nonnegative values of the pharmacokinetic transfer and loss coefficients $A_{12}, A_{21}, A_{13}, A_{31}, A_{11}$ as well as all nonnegative coefficients α, $\mathrm{C_{50}}$, and Q_0.

For our simulation we assume $V_{\rm c} = (0.228$ l/kg$)(M$ kg), where $M = 70$ kg is the mass of the patient, $A_{21}Q_0 = 0.112$ min^{-1}, $A_{12}Q_0 = 0.055$ min^{-1}, $A_{31}Q_0 = 0.0419$ min^{-1}, $A_{13}Q_0 = 0.0033$ min^{-1}, $A_{\rm e}Q_0 = 0.119$ min^{-1}, $a_{\rm eff} = 3.4657$ min^{-1}, $\alpha = 3$, and $\mathrm{C_{50}} = 4$ μg/ml. Note that the parameter values for α and $\mathrm{C_{50}}$ probably exaggerate the effect of propofol on cardiac output. They have been selected to accentuate nonlinearity but they are not biologically unrealistic. Furthermore, to illustrate the proposed neuroadaptive controller we switch the pharmacodynamic parameters $\mathrm{EC_{50}}$ and γ, respectively, from 5.6 μg/ml and 2.39 to 7.2 μg/ml and 3.39 at $t = 15$ min and back to 5.6 μg/ml and 2.39 at $t = 30$ min. Here, we consider noncardiac surgery since cardiac surgery often utilizes hypothermia which itself changes the BIS signal. With $A = \begin{bmatrix} 0 & 1 \\ -1 & -1 \end{bmatrix}$, $L = [0, 1]^{\rm T}$, $\hat{b} = 1$, $Q_{\mathrm{BIS}_1} = 2.0 \times 10^{-4}$ g/min^2, $Q_{\mathrm{BIS}_2} = 4.0 \times 10^{-4}$ g/min^2, $d = 0.005$, and initial conditions $x_1(0) = x_2(0) = x_3(0) = 0$ g, $c_{\rm eff}(0) = 0$ g/ml, $\xi_{\rm c}(0) = [0,\ 0]^{\rm T}$, $\hat{W}_1(0) = 1 \times 10^{-3}[-3_{12\times 1}, 1_{12\times 1}]^{\rm T}$, $\hat{W}_2(0) = 0_{24\times 1}$, Figure 3 shows the concentrations in the central and effect-site compartments versus time. Figure 4 shows actual, noisy, and filtered BIS signals versus time. Finally, Figure 5 shows the effect of using filtered BIS signal on the control signal (propofol infusion rate) versus time.

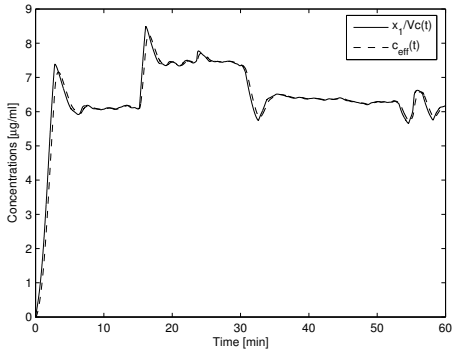

Fig. 3. Concentrations in central and effect site compartments versus time

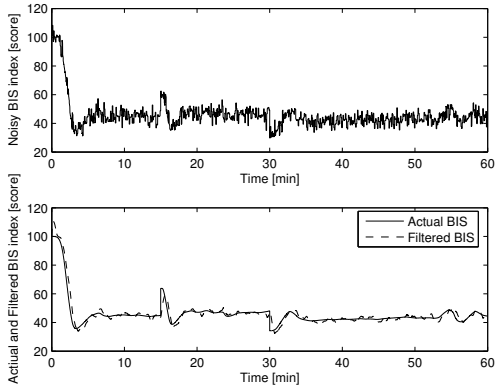

Fig. 4. BIS signal versus time

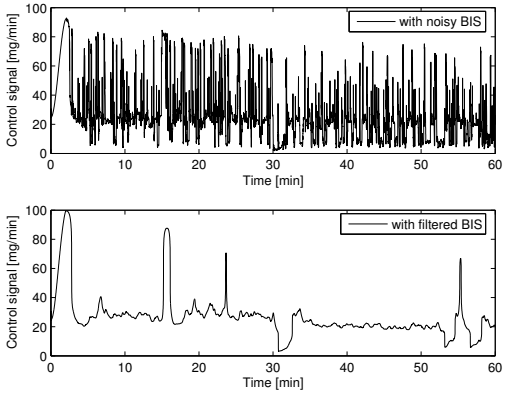

Fig. 5. Control signal (infusion rate) versus time

REFERENCES

[1] R. G. Bickford, "Automatic electroencephalographic control of general anesthesia," *Electroencephalographic Clin. Neurophysiol.*, vol. 2, pp. 93–96, 1950.

[2] H. Schwilden and H. Stoeckel, "Quantitative EEG analysis during anesthesia with isoflurane in nitrous oxide at 1.3 and 1.5 MAC," *Brit. J. Anaesth.*, vol. 59, pp. 738–745, 1987.

[3] P. S. Glass, M. Bloom, L. Kearse, C. Rosow, P. Sebel, and P. Manberg, "Bispectral analysis measures sedation and memory effects of propofol, midazolam, isoflurane, and alfentanil in normal volunteers," *Anesthesiology*, vol. 86, pp. 836–847, 1997.

[4] G. Plourde, "BIS EEG monitoring: What it can and cannot do in regard to unintentional awareness," *Can. J. Anesth.*, vol. 49, p. R12, 2002.

[5] J. W. Johansen and P. S. Sebel, "Development and clinical application of electroencephalographic bispectrum monitoring," *Anesthesiology*, vol. 93, pp. 1336–1340, 2000.

[6] W. M. Haddad, T. Hayakawa, and J. M. Bailey, "Adaptive control for nonnegative and compartmental dynamical systems with applications to general anesthesia," *Int. J. Adapt. Control Signal Process.*, vol. 17, pp. 209–235, 2003.

[7] ——, "Adaptive control for nonlinear compartmental dynamical systems with applications to clinical pharmacology," *Sys. Contr. Lett.*, vol. 55, pp. 62–70, 2006.

[8] W. M. Haddad, J. M. Bailey, T. Hayakawa, and N. Hovakimyan, "Neural network adaptive output feedback control for intensive care unit sedation and intraoperative anesthesia," *IEEE Trans. Neural Networks*, vol. 18, pp. 1049–1066, 2007.

[9] J. Bailey, W. Haddad, J. Im, T. Hayakawa, and P. Nagel, "Adaptive and neural network adaptive control of depth of anesthesia during surgery," in *Proc. Amer. Contr. Conf.*, Minneapolis, MN, 2006, pp. 3409–3414.

[10] E. Lavretsky, N. Hovakimyan, and A. J. Calise, "Upper bounds for approximation of continuous-time dynamics using delayed outputs and feedforward neural networks," *IEEE Trans. Autom. Control*, vol. 48, pp. 1606–1610, 2003.

[11] R. N. Upton, G. I. Ludrook, C. Grant, and A. Martinez, "Cardiac output is a determinant of the initial concentration of propofol after short-term administration," *Aneth. Analg.*, vol. 89, pp. 545–552, 1999.

[12] M. Muzi, R. A. Berens, J. P. Kampine, and T. J. Ebert, "Venodilation contributes to propofol-mediated hypotension in humans," *Aneth. Analg.*, vol. 74, pp. 877–883, 1992.

[13] E. F. Ismail, S. J. Kim, and M. R. Salem, "Direct effects of propofol on myocardial contractility in situ canine hearts," *Anesthesiology*, vol. 79, pp. 964–972, 1992.